

Research



Cite this article: Li D, Wang F, Zhang Z, Jiang W, Zhu Y, Wang Z, Zhang R-Q. 2019 The nature of small molecules adsorbed on defective carbon nanotubes. *R. Soc. open sci.* **6**: 190727. <http://dx.doi.org/10.1098/rsos.190727>

Received: 28 April 2019

Accepted: 22 July 2019

Subject Category:

Chemistry

Subject Areas:

chemical physics/computer modelling and simulation/computational chemistry

Keywords:

physical adsorption, chemical adsorption, defective carbon nanotube, gas molecule

Authors for correspondence:

Zhigang Wang

e-mail: wangzg@jlu.edu.cn

Rui-Qin Zhang

e-mail: aprqz@cityu.edu.hk

This article has been edited by the Royal Society of Chemistry, including the commissioning, peer review process and editorial aspects up to the point of acceptance.

[†]These authors contributed equally to this work.

Electronic supplementary material is available online at <https://dx.doi.org/10.6084/m9.figshare.c.4596242>.



The nature of small molecules adsorbed on defective carbon nanotubes

Danhui Li^{1,2,†}, Fengting Wang^{1,2,†}, Zhiyuan Zhang^{1,2}, Wanrun Jiang^{1,2}, Yu Zhu^{1,2}, Zhigang Wang^{1,2} and Rui-Qin Zhang^{3,4}

¹Institute of Atomic and Molecular Physics, and ²Jilin Provincial Key Laboratory of Applied Atomic and Molecular Spectroscopy, Jilin University, Changchun 130012, People's Republic of China

³Department of Physics, Centre for Functional Photonics (CFP), City University of Hong Kong, Hong Kong SAR, People's Republic of China

⁴Beijing Computational Science Research Center, Beijing 100193, People's Republic of China

ZW, 0000-0002-3028-5196

In this work, we perform a comprehensive theoretical study on adsorption of representative 10-electron molecules H₂O, CH₄ and NH₃ onto defective single-walled carbon nanotubes. Results of adsorption energy and charge transfer reveal the existence of both chemical adsorption (CA) and physical adsorption (PA). While PA processes are common for all molecules, CA could be further achieved by the polar molecule NH₃, whose lone-pair electrons makes it easier to be bonded with the defective nanotube. Our systematic work could contribute to the understanding on intermolecular interactions and the design of future molecular detectors.

1. Introduction

Carbon nanotubes (CNTs), which were discovered in 1991 [1,2], have attracted enduring attention due to their unique structural, thermal, electronic and dynamic properties, which facilitate the use of CNTs in promising medical and biochemical applications. In fact, CNTs have already found applications in many fields, including hydrogen storage [3], free-radicals scavenging activity [4], chemical sensors [5], nanobiology electronics [6], functional groups adsorption substrates [7], capacitors [8] and the like.

The properties of CNTs can be affected strongly by the presence of various defects, which are usually formed during their growth process or caused by the environmental factors. The properties of defective CNTs have been systematically explored in many theoretical and experimental research projects [9–13]. By using scanning gate microscopy (SGM) and scanning impedance

microscopy (SIM), workers have studied the defects in semiconducting single-walled carbon nanotubes (SWCNTs) [12]. Theoretical calculations have shown that local structural defects, such as topological defects, vacancies, impurities and deformations can substantially modify the electronic and transport properties of SWCNTs [13]. Covalent functionalization of SWCNTs with multiplicative biological groups [14–18] based on the effects of the nanotubes' conductive properties, have also been reported [19]. For instance, oxidation-induced defects have been introduced to enhance the sensitivity of an SWCNT to chemical vapours [20]. A five-membered or otherwise configured biological group inserted into the hexagon ring in the SWCNTs has generated apparent chemical reactivity [21]. Also, in the one-dimensional topological defect consisting of octagonal and pentagonal carbon rings inserted into the SWCNT's hexagon, charge transfer [22] and field-effect doping [23] can be applied to manipulate charge carrier concentrations, enabling it to act as a conducting wire [24].

Adsorption of small molecules—such as Xe [25], CF₄ [26], H₂ [27], CH₄ [28], NO [29], NH₃ [30], NO₂ [31] and O₂ [32]—onto SWCNTs, as well as adsorption of H₂O onto graphene [33] or SWCNTs, has been studied theoretically. The sensitivity of SWCNTs to these various small molecules, combined with their own inherent characteristics—such as small size, favourable electrical and mechanical properties, and high surface-area-to-volume ratios, type of defect—have led to many applications for them in various roles as functionalized materials in sensors and in many biological fields. Nevertheless, the complicated, weak interactions between these molecules and carbon materials have been widely reported, but a systematic investigation on the nature of those interactions has been lacking.

A thorough and fundamental theoretical study on small molecules adsorbing on SWCNTs, with a more advanced dispersion force correction, is needed. When a strongly oxidizing defective nanotube interacts with various molecules, it has been found to exhibit different properties from those of the perfect tube. Liu *et al.* reported that reactions replacing reactive sites arise among the 5–1DB defects with the oxynitride on the CNT [34]. Actually, it is easy to chemically bind an acetone onto a Stone–Wales defect or a vacancy of the SWCNT [35]. Such chemical adsorptions (CAs) change the electronic processes and transmission characteristics of the imperfect tube. However, research efforts into the physical adsorption (PA) which is a weak interaction of small molecules, such as H₂O, CH₄ and NH₃, on defective tubes are seldom reported (e.g. the adsorption energy, charge transfer, gap value, dipole moment, etc.).

Previous research studies have examined the adsorption of various molecules on graphene and revealed obviously different characteristics in Raman vibrational and ultraviolet–visible adsorption spectra of the molecules [36]. However, a systematic study on the interaction of specific molecules with different types of defective SWCNTs has yet to be conducted. In this paper, we theoretically study three commonly found representative 10-electron molecules (H₂O, CH₄ and NH₃) adsorbed onto four common defective SWCNT structures. Our results include the various adsorption structures, adsorption energy and charge transfer with the defective structures, compared with those values from the perfect SWCNT. The case of NH₃ is found to be exceptional, because it shows distinct chemical characteristics when it is adsorbed on two types of defective SWCNTs. To elucidate our results, a brief discussion has also been made on the polarity of the small gas molecules in relation to their PA or CA on SWCNTs.

2. Computational methods

The interactions between three representative small molecules (H₂O, CH₄ and NH₃) and four kinds of defective CNTs were studied with the DFTB+ code [37]. Density functional tight-binding (DFTB) is based on DFT and derived from the second-order expansion of the Kohn–Sham total energy functional as calculated within DFT under the standard tight-binding theory [38]. In order to describe the van der Waals (vdW) interaction between the small molecules and defective CNTs, we adopted the DFTB-D method, which is augmented by the empirical London dispersion energy term into the DFTB total energy [39].

The London dispersion energy is given by

$$E_{\text{dis}} = \frac{3}{2} \frac{I_{\alpha} I_{\beta} p_{\alpha} p_{\beta}}{(I_{\alpha} + I_{\beta}) R_{\alpha\beta}^6}, \quad (2.1)$$

$$C_6^{\alpha\beta} = \frac{2C_6^{\alpha} C_6^{\beta} p_{\alpha} p_{\beta}}{p_{\alpha}^2 C_6^{\alpha} + p_{\beta}^2 C_6^{\beta}} \quad (2.2)$$

and

$$C_6^{\alpha} = 0.75 \sqrt{N_{\alpha} p_{\alpha}^3}, \quad (2.3)$$

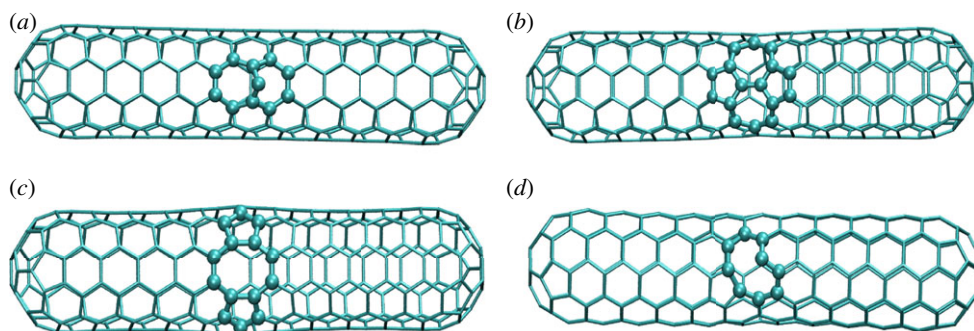


Figure 1. The structures of the four types of defective CNTs studied. The SWCNTs had the following defects: (a) an ad-atom (a), (b) a chiral Stone–Wale defect (b), (c) two missing C atoms (c) and (d) a monovacancy defect (d).

where N_α is the Slater–Kirkwood effective number of electrons. The $1/R^6$ dependence is truncated for small interatomic distances with an appropriate damping function [40]. This method has been successfully used to study organic molecules interacting with materials [41], the adsorption of water clusters on a graphene surface [42] and so forth.

To ensure the reliability of calculations, the cases of defective nanotubes with and without the cap at both ends were also considered. All of our results for the capped defective and perfect nanotubes adsorbed with CH_4 , H_2O and NH_3 calculated with DFTB were verified with density functional theory (DFT) calculations using PBE0-D3 functional [43,44] and 6–31 g (d, p) basis set. Conventional DFT fails in the study of weak interactions, but a newly developed method—density functional theory with empirical dispersion corrections (DFT-D)—can yield more trustworthy results. The results with DFT-D are superior because the method can compute the long-range force part, which gives more accurate data in dealing with the point charge Coulomb interaction among long-range parts; thus, it can describe PA more accurately. However, DFTB-D has an efficiency advantage in comparison with DFT-D, which is conducive to the study of more complex systems [45].

3. Results and discussion

In this work, we consider the interactions of H_2O , CH_4 and NH_3 with the pure (5, 5) SWCNT (marked with letter ‘p’) and four types of defective CNTs. The denotations of the four defective nanotubes are ‘a’ for ad-atom, ‘b’ for a chiral Stone–Wales (SW) defect, ‘c’ for the case of two missing C-atoms and ‘d’ for a monovacancy defect, respectively. The configurations of the CNTs with defects are presented in figure 1. There are several conformations of the same molecule adsorbed on the various CNTs. With different initial molecular–CNT conformations, we obtained 15 stable structures that are based on a large number of different initial conformations and are shown in figure 2. The results show that CA occurred when NH_3 adsorbed on ‘a’ and ‘d’ defective nanotubes, as shown in figure 2a. In figure 2b, the conformations for the PA case are shown. We can see several stable structures with a hydrogen atom pointing to the nanotube, which is similar with the anion– π interaction reported in the literature [46]. It should be noted that, for all the adsorbates, it is the proton instead of the heavy atom (N or O) that is pointing to the CNTs. This is because their electrons are sp^3 hybridized, indicating that electron lone pairs exist in the ‘proton-free’ directions. Such electron-negative lone pair would repulse either with the lone pairs of the dangling C or the π electrons, causing instability of the system, contrary to the electron-relative protons.

However, NH_3 adsorbed onto the perfect CNT reveals different properties from those of the other molecules, with the N atom staying close to the nanotube. That observation is concordant with the findings of Shirvani *et al.* [47]. In these structures, we readily found that one C atom is not coplanar with other atoms on the same six-membered rings in the ‘a’ and ‘d’ types of defective tubes, unlike the case with the ‘b’ and ‘c’ types. The structure of CH_4 differs in that one H atom pointing to the CNT appears in the ‘a’ and ‘d’ tubes and three H stable structures, and when H_2O adsorbs on ‘a’ defective nanotube, the distance is the smallest. Atoms pointing to the CNT appear in the ‘b’ and ‘c’ tubes, as is the case with the ‘p’ tube. To summarize, we obtain different stable structures when the same molecule is adsorbed onto the various CNTs. Comparing the stable structures of the PA cases, we concluded that the distance of the CH_4 to ‘c’ defective nanotubes is the largest in all of the angles which measure the deviations of the small molecules from the x -axis. When H_2O and NH_3 adsorb on ‘b’ defective nanotubes, the angles are larger; however, when CH_4 and H_2O adsorb on ‘d’ defective

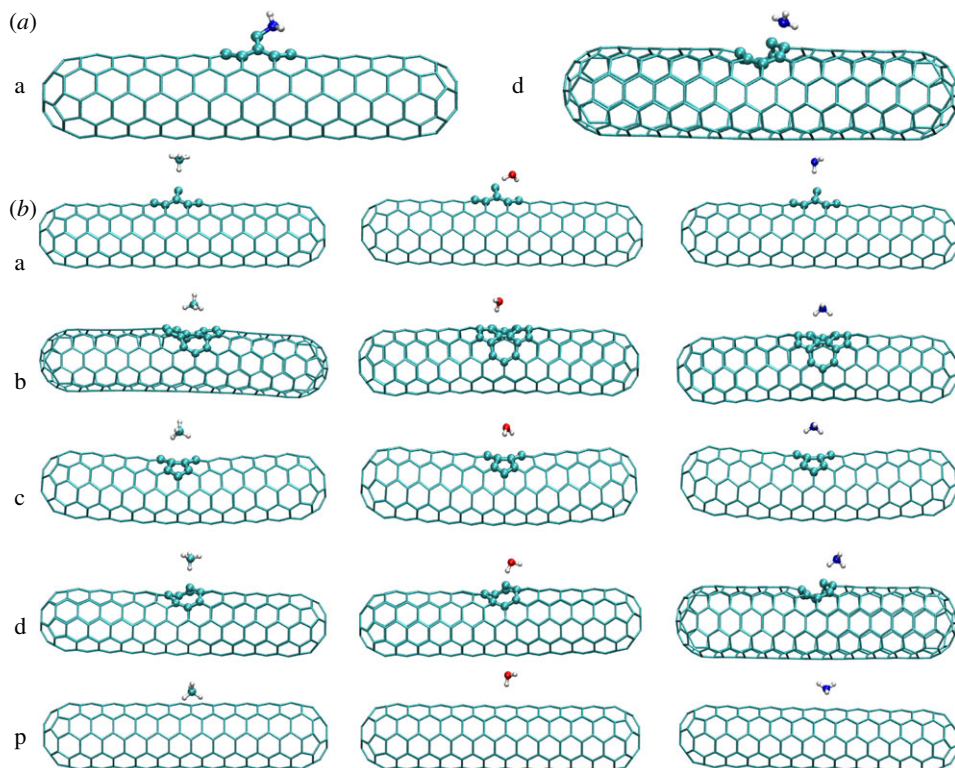


Figure 2. (a) The optimized configurations of NH₃ adsorbed on the ‘a’ and ‘d’ defective nanotubes for the chemical case. (b) The optimized configurations of the small molecules (CH₄, NH₃, H₂O) adsorbed on the ‘a’ ‘b’ ‘c’ ‘d’ defective and perfect nanotubes for the physical case.

and perfect nanotubes, the angles are the smallest. The data of all stable structures are provided in the electronic supplementary material.

The results of our calculations indicate that the NH₃ molecule behaves differently from the others. The NH₃ molecule exhibits both PA and CA adsorption on the ‘a’ and ‘d’ type CNTs for the different structures of the ‘a’ and ‘d’ defective nanotubes from other types, with the lone-pair electrons of the top defective C-atoms in ‘a’ and ‘d’ being more easily bonded with small molecules. By contrast, in the other defective ‘b’ and ‘c’ defective nanotubes, three electrons in the outer shell of the defective C-atoms bond with other C-atoms and the last electron forms π bonds. As for the polar molecule NH₃, the N-atom in the NH₃ takes the inequivalent sp³ hybridization forming three σ bonds and one lone-pair electrons, making it is easier to bond with ‘a’ and ‘d’ defective nanotubes to form the stable structure as shown in figure 2a. However, the H₂O and CH₄ molecules show only PA interactions. Among them, CH₄ is non-polar molecule with the C-atom taking sp³ equivalent hybridization and involving no lone-pair electrons while there are two lone-pair electrons in H₂O, making the structures of ‘a’ and ‘d’ defective nanotubes less stable.

Figure 3 reveals the direction of the charge transfer clearly for the CA case in ‘a’ and ‘d’ defective nanotubes. We can see in figure 3a the electron density difference of ‘a’ and ‘d’ defective nanotubes adsorbed with NH₃.

The isovalues of the isosurfaces are 0.004 and -0.004 , respectively, for the pink and green area; the pink areas on the defective CNTs represent the electron increase but the green area expresses the charge decrease. The figures show that near the ‘a’ and ‘d’ defective CNTs the pink area is larger, revealing the direction of charge transfer to be from the defective CNTs to NH₃. That result is consistent with the electron density difference integral as shown in figure 3b, which is obtained by integrating the electron density in the y and z direction onto the x -direction, following $I(x) = \int_{-\infty}^{+\infty} \rho(x,y,z)dydz$. In figure 3b, the vertical axis represents the integrated electron density difference and the horizontal axis is the coordinate x , ranging from 3 to 13 Å. The N atom is at $x = 9.06$ Å for ‘a’ defective nanotube and 9.27 Å for ‘d’ as shown in the electronic supplementary material, figure S1. The vertical coordinates of the points above zero represent the increment of the electron density and below zero the decrement of the electron density. We obtain the same conclusion that the charge transfer is from ‘a’ and ‘d’ defective nanotubes to NH₃.

In table 1, the CA values are larger than the PA values for both the adsorption energy and the charge transfer of NH₃ adsorbed on the ‘a’ and ‘d’ type CNTs. More specifically, the charge transfer for the

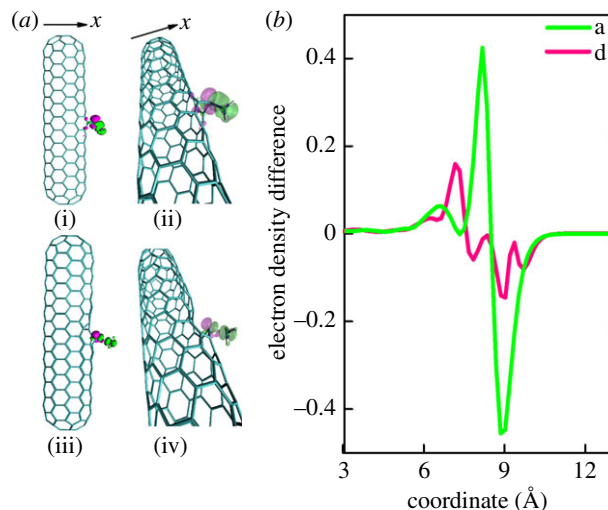


Figure 3. (a) The electron density difference of the ‘a’ and ‘d’ defective nanotubes adsorbed with NH_3 molecule for the CA case. (i and ii) The front and side figures of the electron density difference when NH_3 adsorbed on ‘a’ defective nanotube. (iii and iv) The front and side figures of the electron density difference when NH_3 is adsorbed on ‘d’ defective nanotube. (b) The electron density difference integral for the chemical adsorption that ‘a’ and ‘d’ defective nanotubes adsorbed with NH_3 .

Table 1. The binding energies ΔE , the charge transfer Q of NH_3 adsorbed on ‘a’ and ‘d’ type defect CNTs for the PA and the CA, respectively.

tube	PA		CA	
	ΔE (meV)	Q (e)	ΔE (meV)	Q (e)
a	−78	−0.01	−1260	0.66
d	−68	0	−461	0.27

CA case is of the order of 10^{-1} e, showing a significant contrast with 10^{-3} e for the PA. Both of the adsorption energies for the CA cases of ‘a’ and ‘d’ defects are of the order of 10^3 meV and 10^2 meV, whereas the adsorption energy of both the ‘a’ and ‘d’ defects is of the order of 10^1 meV for the PA case. However, the adsorption energy and charge transfer for adsorption on ‘a’ defective nanotube is larger than ‘d’ defective nanotube, especially for CA, for the difference of the defective C-atoms that the top defective C-atom of ‘a’ is most distant from the principle axis of the nanotube among the defective and perfect nanotubes, which makes NH_3 more easily polarized and bonded when adsorbed on ‘a’ defective nanotube.

Compared with the CA, the adsorption energy and the charge transfer of H_2O , CH_4 and NH_3 on the CNTs we calculated are much less, as shown in figure 4. The calculated PA energies vary within 400 meV. Moreover, all of them are around 100 meV except the case when H_2O adsorbed on ‘a’ defective nanotube (321 meV). To verify the differences of this phenomenon, further electronic density and the local density of state (LDOS) analyses are carried out. It turns out that not only the electron density of the H_2O adsorption in the intermolecular area is obviously larger than those of NH_3 and CH_4 , but its LDOS also presents delocalization of the orbitals through the region. It could be concluded that the interaction feature of this system is not simply van de Waals intermolecular interaction (detailed information is included in the electronic supplementary material). Figure 4 also presents the charge transfers for each of the configurations. The green values represent the direction of the charge transfer that shows an electron transfer from the defective or perfect nanotubes to the small molecules (i.e. CH_4 , H_2O and NH_3).

Actually, the activation energy of desorption and the binding energies for small molecules adsorbed on carbon-based materials have been systematically observed in the previous experimental research [48]. The binding energy of small molecules with SWCNT is of similar magnitude to that of the PA cases above. This could also prove the reliability of our results.

Correspondingly, the pink values denote the opposite direction. It shows that the charge transfer from the perfect nanotube to NH_3 is of the order of 10^{-2} e. The same amount of charge transfer number is found from the NH_3 to a defective nanotube, whereas for other systems the charge transfer is almost

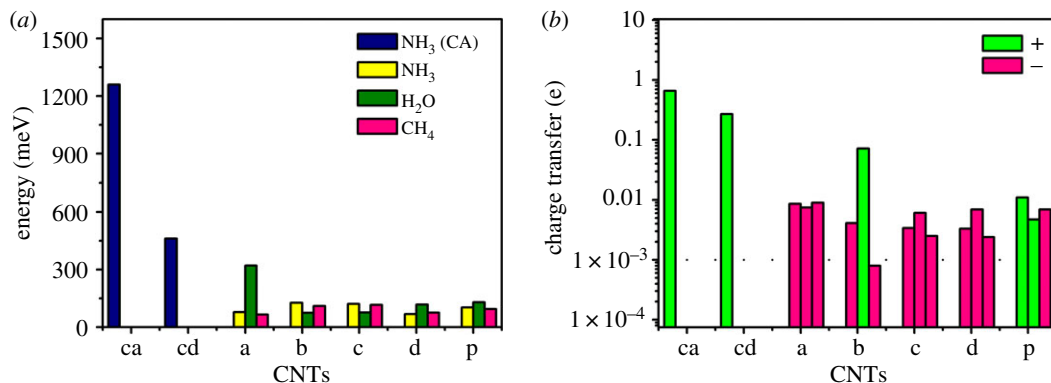


Figure 4. (a) The comparison of the physical and chemical adsorption energies, CA structures (blue), PA structures NH₃ (yellow), H₂O (olive), CH₄ (pink). (b) The comparison of the charge transfer of the PA and CA. The green (or pink) colour denotes the electron decrease (increase) or the charge increase (decrease).

negligible. The charge transfer from 'a' defective nanotube to H₂O is approximately 10^{-1} e. It is because of the lone-pair electrons of the top defective C-atom of 'a' which is the most distant from the principle axis of the nanotube among the defective and perfect nanotubes. Also, H₂O is polar molecular with sp³ non-equivalent hybridization and the two lone-pair electrons make it easily adsorbed on the defective nanotubes especially on 'a' defective nanotube.

Furthermore, calculation of the cases for CNTs without the 'cap' were also carried out. The results show that when the 'cap' of the defective nanotubes is removed, the calculations still support the similar conclusions for the chemical case and PA cases, except for the 'c' defective nanotube whose band gap becomes larger when the cap is removed.

In order to show the electronic density-based properties of the adsorption structure, electronic density difference analyses under DFT method were carried out. As expected, electronic density differences of the CA structures are much larger than those of the PA ones, consistent with the results of charge transfer analyses above. The details of electronic density difference are provided in the electronic supplementary material.

Furthermore, we also calculated the energies of all the dissociative adsorption cases with DFTB-D. By comparing the energies of all dissociative adsorptions stable structures with the corresponding coordination complexes, we concluded that dissociative adsorptions for 'a' and 'd' defective nanotubes are possible and further calculated their adsorption energies. The comparison of their local density states is also provided, from which we can see that the distribution of the density states is more uniform in the dissociative adsorption ones than the coordination complexes, and the delocalization of the orbital is weaker. We also performed molecular dynamic simulations of the possible dissociative adsorption cases. All the simulations were performed at room temperature. However, we have not observed any dissociative adsorptions, indicating that they do not easily occur. All the figures of the structures and energy data are provided in the electronic supplementary material.

Besides, there are many studies in the literature certifying the accuracy of the DFTB method which is compared favourably with DFT [36,45,49,50]. And the 'd' defective nanotubes adsorbed chemically with NH₃ calculated with DFT have been reported [30], which confirms the results of our work further. The comparisons of the adsorption energies and charge transfer values of the CA cases in which NH₃ adsorbs on the 'a' and 'd' defective nanotubes calculated with DFTB and DFT are provided in the electronic supplementary material, tables S1 and S2. We obtained the same conclusions that there are obvious charge transfer and much larger adsorption energy when NH₃ adsorbs on the 'a' and 'd' defective nanotubes chemically. Because of the similarity in the results obtained with DFT and DFTB (the calculation speed of DFTB is three magnitudes faster than DFT), it can be used in the simulation and calculation of large molecules system [41,51] in the future.

4. Conclusion

In this work, we systematically studied the adsorption between common 10-electron small molecules and CNTs with different defects. The reliability of the results is ensured by comparing the DFTB and DFT methods. Our calculated adsorption energy, charge transfer, energy gap and dipole moment of the studied systems reveal that PA is the common process, except with NH₃, which undergoes both PA and

CA due to its large polarity and apparent charge transfer. CA occurs for NH_3 on the defective 'a' and 'd' defective nanotube involving considerable adsorption energies and charge transfer because NH_3 can be easily polarized. On the contrary, PAs take place for other small molecules such as CH_4 , H_2O and NH_3 on the 'a', 'b', 'c', 'd' defective and perfect nanotubes with negligible adsorption energies and charge transfer.

The interactions that we determine between those gas molecules and the defective nanotubes are very important for identifying a specific gas such as NH_3 based on the obvious different charge transfer and adsorption energies of the CA and PA. The mechanism can be used to fabricate gas sensors, as the conductivity of defective CNTs affected by the CA. Furthermore, the obtained consistency of DFTB and DFT calculations has proved the reliability of the highly efficient DFTB method. This would be helpful for us to conduct large-scale calculations and extend research to more complicated systems.

Data accessibility. Additional data are available in the electronic supplementary material.

Authors' contributions. D.L. and F.W. performed simulations. Z.W. and R-Q.Z. conceived this project. D.L., Z.Z., W.J. and Y.Z. analysed results. D.L. produced the figures. D.L., Z.Z., R-Q.Z. and Z.W. wrote the paper. All authors commented on the manuscript.

Competing interests. We declare we have no competing interests.

Funding. The work described in this paper is supported by grants from the National Science Foundation of China (under grant no. 11674123).

Acknowledgements. We thank Miss Sonam Wangmo, Mr Jianpeng Wang, Weiyu Xie, Drs Yan Meng, Minsi Xin, Ruixia Song and Bolong Huang for the stimulating discussions. We also acknowledge the High Performance Computing Center (HPCC) of Jilin University for computation resources.

References

- Iijima S. 1991 Helical microtubules of graphitic carbon. *Nature* **354**, 56–58. (doi:10.1038/354056a0)
- Iijima S, Ichihashi T. 1993 Single-shell carbon nanotubes of 1-nm diameter. *Nature* **363**, 603–605. (doi:10.1038/363603a0)
- Liu C, Fan YY, Liu M, Cong HT, Cheng HM, Dresselhaus MS. 1999 Hydrogen storage in single-walled carbon nanotubes at room temperature. *Science* **286**, 1127–1129. (doi:10.1126/science.286.5442.1127)
- Martinez A, Galano A. 2010 Free radical scavenging activity of ultrashort single-walled carbon nanotubes with different structures through electron transfer reactions. *J. Phys. Chem. C* **114**, 8184–8191. (doi:10.1021/jp100168q)
- Kong J, Franklin NR, Zhou C, Chapline MG, Peng S, Cho K, Dai H. 2000 Nanotube molecular wires as chemical sensors. *Science* **287**, 622–625. (doi:10.1126/science.287.5453.622)
- Katz E, Willner I. 2004 Biomolecule-functionalized carbon nanotubes: applications in nanobioelectronics. *Chemphyschem* **5**, 1084–1104. (doi:10.1002/cphc.200400193)
- Zhang X *et al.* 2017 Highly selective and active CO_2 reduction electrocatalysts based on cobalt phthalocyanine/carbon nanotube hybrid structures. *Nat. Commun.* **8**, 14675. (doi:10.1038/ncomms14675)
- Gong W *et al.* 2018 Carbon nanotubes and manganese oxide hybrid nanostructures as high performance fiber supercapacitors. *Commun. Chem.* **1**, 16. (doi:10.1038/s42004-018-0017-z)
- Hashimoto A, Suenaga K, Gloter A, Urita K, Iijima S. 2004 Direct evidence for atomic defects in graphene layers. *Nature* **430**, 870–873. (doi:10.1038/nature02817)
- Lusk MT, Carr LD. 2008 Nanoengineering defect structures on graphene. *Phys. Rev. Lett.* **100**, 175 503–175 506. (doi:10.1103/PhysRevLett.100.175503)
- Meyer JC, Kisielowski C, Emi R, Rossell MD, Crommie MF, Zettl A. 2008 Direct imaging of lattice atoms and topological defects in graphene membranes. *Nano Lett.* **8**, 3582–3586. (doi:10.1021/nl801386m)
- Freitag M, Johnson AT, Kalinin SV, Bonnell DA. 2002 Role of single defects in electronic transport through carbon nanotube field-effect transistors. *Phys. Rev. Lett.* **89**, 216801. (doi:10.1103/PhysRevLett.89.216801)
- Chico L, López Sancho MP, Muñoz MC. 1998 Carbon-nanotube-based quantum dot. *Phys. Rev. Lett.* **81**, 1278–1281. (doi:10.1103/PhysRevLett.81.1278)
- Chen J, Hamon MA, Hu H, Chen Y, Rao AM, Eklund PC, Haddon RC. 1998 Solution properties of single-walled carbon nanotubes. *Science* **282**, 95–98. (doi:10.1126/science.282.5386.95)
- Bahr JL, Yang J, Kosynkin DV, Bronikowski MJ, Smalley RE, Tour JM. 2001 Functionalization of carbon nanotubes by electrochemical reduction of aryl diazonium salts: a bucky paper electrode. *J. Am. Chem. Soc.* **123**, 6536–6542. (doi:10.1021/ja010462s)
- Holzinger M, Vostrowsky O, Hirsch A, Hennrich F, Kappes M, Weiss R, Jellen F. 2001 Sidewall functionalization of carbon nanotubes. *Angew. Chem. Int. Ed.* **40**, 4002–4005. (doi:10.1002/1521-3773(20011105)40:21<4002::AID-ANIE4002>3.0.CO;2-8)
- Georgakilas V, Kordatos K, Prato M, Guldi DM, Holzinger M, Hirsch A. 2002 Organic functionalization of carbon nanotubes. *J. Am. Chem. Soc.* **124**, 760–761. (doi:10.1021/ja016954m)
- Dyke CA, Tour JM. 2003 Solvent-free functionalization of carbon nanotubes. *J. Am. Chem. Soc.* **125**, 1156–1157. (doi:10.1021/ja0289806)
- Zhao J, Park H, Han J, Lu JP. 2004 Electronic properties of carbon nanotubes with covalent sidewall functionalization. *J. Phys. Chem. B* **108**, 4227–4230. (doi:10.1021/jp036814u)
- Bower C, Rosen R, Jin L, Han J, Zhou O. 1999 Deformation of carbon nanotubes in nanotube-polymer composites. *Appl. Phys. Lett.* **74**, 3317–3319. (doi:10.1063/1.123330)
- Hirsch A. 2002 Functionalization of single-walled carbon nanotubes. *Angew. Chem. Int. Ed.* **41**, 1853–1859. (doi:10.1002/1521-3773(20020603)41:11<1853::AID-ANIE1853>3.0.CO;2-N)
- Jung N, Kim N, Jockusch S, Turro NJ, Kim P, Brus L. 2009 Charge transfer chemical doping of few layer graphenes: charge distribution and band gap formation. *Nano Lett.* **9**, 4133–4137. (doi:10.1021/nl902362q)
- Zhang Y, Tang T-T, Girit C, Hao Z, Martin MC, Zettl A, Crommie MF, Shen YR, Wang F. 2009 Direct observation of a widely tunable bandgap in bilayer graphene. *Nature* **459**, 820–823. (doi:10.1038/nature08105)
- Lahiri J, Lin Y, Bozkurt P, Oleynik II, Batzill M. 2010 An extended defect in graphene as a metallic wire. *Nat. Nanotechnol.* **5**, 326–329. (doi:10.1038/nnano.2010.53)
- Kuznetsova A, Yates Jr JT, Liu J, Smalley RE. 2000 Physical adsorption of xenon in open single walled carbon nanotubes: observation of a quasi-one-dimensional confined Xe phase. *J. Chem. Phys.* **112**, 9590–9598. (doi:10.1063/1.481575)
- Byl O, Kondratyuk P, Forth ST, FitzGerald SA, Chen L, Johnson JK, Yates JT. 2003 Adsorption of CF_4 on the internal and external surfaces of opened single-walled carbon nanotubes: a vibrational spectroscopy study. *J. Am. Chem. Soc.* **125**, 5889–5896. (doi:10.1021/ja020949g)

27. Dillon AC, Heben MJ. 2001 Hydrogen storage using carbon adsorbents: past, present and future. *Appl. Phys. A* **72**, 133–142. (doi:10.1007/s003390100788)
28. Lubezky A, Chechelintsky L, Folman M. 1996 IR spectra of CH₄, CD₄, C₂H₄, C₂H₂, CH₃OH and CH₃OD adsorbed on C₆₀ films. *J. Chem. Soc. Faraday Trans.* **92**, 2269–2274. (doi:10.1039/ft9969202269)
29. Fastow M, Kozirovski Y, Folman M, Heidberg J. 1992 IR spectra of carbon monoxide and nitric oxide adsorbed on fullerene (C₆₀). *J. Phys. Chem.* **96**, 6126–6128. (doi:10.1021/j100194a008)
30. Oliva C, Strodel P, Goldbeck-Wood G, Maiti A. 2008 Understanding the interaction of ammonia with carbon nanotubes. *NSTI Nanotech* **3**, 655–658.
31. Porto AB, de Oliveira LFC, Dos Santos HF. 2016 Exploring the potential energy surface for reaction of SWCNT with NO₂⁺: a model reaction for oxidation of carbon nanotube in acid solution. *Comput. Theor. Chem.* **1088**, 1–8. (doi:10.1016/j.comptc.2016.05.002)
32. Li J, Lu Y, Ye Q, Cinke M, Han J, Meyyappan M. 2003 Carbon nanotube sensors for gas and organic vapor detection. *Nano Lett.* **3**, 929–933. (doi:10.1021/nl034220x)
33. Zhanpeisov NU, Zhidomirov GM, Fukumura H. 2009 Interaction of a single water molecule with a single graphite layer: an integrated ONIOM study. *J. Phys. Chem. C* **113**, 6118–6123. (doi:10.1021/jp810460b)
34. Liu LV, Tian WQ, Wang YA. 2006 Chemical reaction of nitric oxides with the 5-1DB defect of the single-walled carbon nanotube. *J. Phys. Chem. B* **110**, 1999–2005. (doi:10.1021/jp053931b)
35. Chakrapani N, Zhang YM, Nayak SK, Moore JA, Carroll DL, Choi YY, Ajayan PM. 2003 Chemisorption of acetone on carbon nanotubes. *J. Phys. Chem. B* **107**, 9308–9311. (doi:10.1021/jp034970v)
36. Meng Y *et al.* 2013 Signatures in vibrational and UV-visible absorption spectra for identifying cyclic hydrocarbons by graphene fragments. *Nanoscale* **5**, 12 178–12 184. (doi:10.1039/c3nr02933f)
37. Elstner M, Porezag D, Jungnickel G, Elsner J, Haugk M, Frauenheim T, Suhai S, Seifert G. 1998 Self-consistent-charge density-functional tight-binding method for simulations of complex materials properties. *Phys. Rev. B* **58**, 7260–7268. (doi:10.1103/PhysRevB.58.7260)
38. Frauenheim T, Seifert G, Elsterner M, Hajnal Z, Jungnickel G, Porezag D, Suhai S, Scholz R. 2000 A self-consistent charge density-functional based tight-binding method for predictive materials simulations in physics, chemistry and biology. *Phys. Status Solidi B* **217**, 41–62. (doi:10.1002/(SICI)1521-3951(200001)217:1<41::AID-PSSB41>3.0.CO;2-V)
39. Elstner M, Hobza P, Frauenheim T, Suhai S, Kaxiras E. 2001 Hydrogen bonding and stacking interactions of nucleic acid base pairs: a density-functional-theory based treatment. *J. Chem. Phys.* **114**, 5149–5155. (doi:10.1063/1.1329889)
40. Lin CS, Zhang RQ, Niehaus TA, Frauenheim T. 2007 Geometric and electronic structures of carbon nanotubes adsorbed with flavin adenine dinucleotide: a theoretical study. *J. Phys. Chem. C* **111**, 4069–4073. (doi:10.1021/jp068846y)
41. Elstner M, Frauenheim T, Kaxiras E, Seifert G, Suhai S. 2000 A self-consistent charge density-functional based tight-binding scheme for large biomolecules. *Phys. Status Solidi B* **217**, 357–376. (doi:10.1002/(SICI)1521-3951(200001)217:1<357::AID-PSSB357>3.0.CO;2-J)
42. Lin CS, Zhang RQ, Lee ST, Elstner M, Frauenheim T, Wan LJ. 2005 Simulation of water cluster assembly on a graphite surface. *J. Phys. Chem. B* **109**, 14 183–14 188. (doi:10.1021/jp050459l)
43. Perdew JP, Burke K, Ernzerhof M. 1996 Generalized gradient approximation made simple. *Phys. Rev. Lett.* **77**, 3865. (doi:10.1103/PhysRevLett.77.3865)
44. Adamo C, Barone V. 1999 Toward reliable density functional methods without adjustable parameters: the PBE0 model. *J. Chem. Phys.* **110**, 6158–6170. (doi:10.1063/1.478522)
45. Zheng G, Irlé S, Morokuma K. 2005 Performance of the DFTB method in comparison to DFT and semiempirical methods for geometries and energies of C₂₀–C₈₆ fullerene isomers. *Chem. Phys. Lett.* **412**, 210–216. (doi:10.1016/j.cpllett.2005.06.105)
46. Ma JC, Dougherty DA. 1997 The cation– π interaction. *Chem. Rev.* **97**, 1303–1324. (doi:10.1021/cr9603744)
47. Shirvani BB, Beheshtian J, Parsafar G, Hadipour NL. 2010 DFT study of NH₃(H₂O)_{n=0,1,2,3} complex adsorption on the (8, 0) single-walled carbon nanotube. *Comput. Mater. Sci.* **48**, 655–657. (doi:10.1016/j.commatsci.2010.02.035)
48. Ulbricht H, Zacharia R, Cindir N, Hertel T. 2006 Thermal desorption of gases and solvents from graphite and carbon nanotube surfaces. *Carbon* **44**, 2931–2942. (doi:10.1016/j.carbon.2006.05.040)
49. Elstner M, Jalkanen KJ, Knapp-Mohammady M, Frauenheim T, Suhai S. 2001 Energetics and structure of glycine and alanine based model peptides: approximate SCC-DFTB, AM1 and PM3 methods in comparison with DFT, HF and MP2 calculations. *Chem. Phys.* **263**, 203–219. (doi:10.1016/S0301-0104(00)00375-X)
50. Kotakoski J, Krashenninnikov AV, Nordlund K. 2006 Energetics, structure, and long-range interaction of vacancy-type defects in carbon nanotubes: atomistic simulations. *Phys. Rev. B* **74**, 245420. (doi:10.1103/PhysRevB.74.245420)
51. Li H-B, Page AJ, Hettich C, Aradi B, Kohler C, Frauenheim T, Irlé S, Morokuma K. 2014 Graphene nucleation on a surface-molten copper catalyst: quantum chemical molecular dynamics simulations. *Chem. Sci.* **5**, 3493–3500. (doi:10.1039/C4SC00491D)